JP Journal of Heat and Mass Transfer

http://www.pphmj.com
http://dx.doi.org/10.17654/0973576323035
Volume 34, 2023, Pages 105-126 **P-ISSN: 0973-5763**

HALL AND HEAT SOURCE EFFECTS OF FLOW PAST A PARABOLIC ACCELERATED ISOTHERMAL VERTICAL PLATE IN THE PRESENCE OF CHEMICAL REACTION AND RADIATION

D. Lakshmikaanth[1,2], A. Selvaraj[1,*], P. Selvaraju[3] and S. Dilip Jose[4]

[1]Department of Mathematics
Vels Institute of Science, Technology and Advanced Studies
Chennai-600117, India
e-mail: aselvaraj_ind@yahoo.co.in

[2]College of Fish Nutrition and Food Technology
Tamilnadu Dr. J. Jayalalithaa Fisheries University
Chennai-600051, Tamil Nadu, India
e-mail: lakshmikanth@tnfu.ac.in

[3]Department of Mathematics
Rajalakshmi Institute of Technology
Chennai-600124, Tamil Nadu, India

[4]Department of Mathematics
Periyar Maniammai Institute of Science and Technology
(Deemed-to-be University)
Vallam 613403, Thanjavur, Tamil Nadu, India

Received: January 10, 2023; Revised: June 5, 2023; Accepted: June 10, 2023
Keywords and phrases: Hall current, radiation, heat source, MHD, chemical reaction.
*Corresponding author

How to cite this article: D. Lakshmikaanth, A. Selvaraj, P. Selvaraju and S. Dilip Jose, Hall and heat source effects of flow past a parabolic accelerated isothermal vertical plate in the presence of chemical reaction and radiation, JP Journal of Heat and Mass Transfer 34 (2023), 105-126. http://dx.doi.org/10.17654/0973576323035

Published Online: July 14, 2023

Abstract

We study Hall current, heat source with radiation and chemical reaction of first order viscous fluid flow, incompressible fluid with heat and mass transfer past an accelerated isothermal vertical plate. The inverse Laplace transform technique is used to solve the ascendant mathematical statement. The numerical values are given after our study of the acceleration, thermal reading and adsorption for certain parameters, including thermal Grashof number, Prantdl number, Schmidt number, and mass Grashof number. Based on the study, we found out that the velocity of the fluid increases with increase in heat, Hall current as well as Grashof value and it decreases with increase in radiation. Concentration reduces when chemical reaction increases.

1. Introduction

The evaluation of fluid movement is an important part of the reactor heat transfer as it can be used to a wide range of systems, including biological systems, household appliances, homes and businesses, industrial operations, and food preparation like electronic equipment cooling, formation of heating and coolant systems, refrigeration of food among many others. Das et al. [1] studied how a first order homogeneous chemical reaction would alter an irregular fluid flow. Muthukumaraswamy [2] made a similar study regarding how the change in reaction affects the velocity. Sarki and Ahmed [3] also made similar study and found that the velocity of fluid increases with increase in Gr, K, t and Gc, while Thamizhsudar et al. [4] observed that axial velocity increases with increase in Hall parameter, mass as well as Grashof number. Dilip Jose and Selvaraj [5] found that the velocity increases with increase in Gr and Gc. Uwanta and Sani [6] analyzed how the parameters of the thermal Gr, Gc, t and the variable of thermal conductivity cause velocities to rise while the parameters of the Pr, Sc, R, k and magnetic field cause velocities to decrease. While temperature reduces with increasing Prandtl number, radiation, and suction factors, it rises with increase in thermal conductivity and heat source characteristics. With increase in Sc and

k, the concentration reduces. Maran et al. [7] presented graphical estimation of temperature, float speed which clearly conveys that an executed attractive region's tendency edge increases with declining speed. Rachna [8] carried a fine theoretical work obtaining the velocity to rise with increase in Gr and Gc. The impacts of the non-uniform heat parameter on dynamics are depicted in chart by Abel and Mahesha [9]. The numerical technique on several parameters of heat radiation was obtained by Ferdows et al. [10]. The Hall current effect on unsteady hydromagnetic flow was studied by Acharya et al. [11]. Siddheshwar and Mahabaleshwar [12] talked about how heat transport over a stretched sheet and MHD flow of a viscoelastic liquid is affected by radiation and heat sources. Sharma and Singh [13] described how heat-generating system is subjected to a transverse magnetic field. Muthucumaraswamy and Geetha [14] investigated the parabolic motion effects on an isothermal vertical plate. The inverse Laplace transform is solved in Hetnarski's Zastosowania Metamatikyki VII paper [15, 16].

2. Numerical Formulation

Here, we assume viscous, incompressible fluid that conducts current flowing past an infinite plate that is located in the plane $z = 0$. The y-axis is normal to other axes, while x-axis is measured in the object's drift order. This plate is parabolic accelerated along the x-axis with a velocity of $q = t^2$. The plate in this instance is not electrically conductive. In the flow field, the pressure is uniform as well. The continuity equation notes the elements of 'F' velocity vector. $w' = 0$ is satisfied when $F = 0$ results in $w' = 0$ everywhere in the flow. Here, just z and t determine the flow volumes. The following equations regulate the unsteady flow under these presumptions:

$$\frac{\partial u^*}{\partial t^*} = \vartheta \frac{\partial^2 u^*}{\partial z^{*2}} + g\beta(T^* - T_\infty^*) + g\beta(C^* - C_\infty^*) - \frac{\sigma B_0^2 \mu^2 (u^* + m_1 v^*)}{\rho(1 + m_1^2)}, \quad (1)$$

$$\frac{\partial v^*}{\partial t^*} = \vartheta \frac{\partial^2 u^*}{\partial z^{*2}} + \frac{\sigma B_0^2 \mu^2 (m_1 u^* - v^*)}{\rho(1 + m_1^2)}, \quad (2)$$

$$\frac{\partial \theta^*}{\partial t^*} = \frac{1}{Pr}\frac{\partial^2 \theta^*}{\partial z^{*2}} - R\theta^* + Q\theta^*, \tag{3}$$

$$\frac{\partial C^*}{\partial t^*} = \frac{1}{Sc}\frac{\partial^2 C^*}{\partial z^{*2}} - kC^*. \tag{4}$$

The boundary conditions are

$$u^* = 0,\ v^* = 0,\ T^* = T_\infty^*,\ C^* = C_\infty^* \text{ at } t_\infty^* \le 0, \text{ for every } z_\infty \le 0,$$

$$u^* = t^{*2},\ T^* = T_\infty^*,\ C^* = C_\infty^* \text{ at } t^* > 0 \text{ for } z^* = 0,$$

$$u^* \to 0,\ T^* \to T_\infty^*,\ C^* \to C_\infty^* \text{ at } z_\infty^* \to \infty. \tag{5}$$

The consequent dimensionless aggregate is:

$$U = \frac{u^*}{(Vu_0)^{\frac{1}{3}}},\ V = \frac{v^*}{(Vu_0)^{\frac{1}{3}}},\ t = t^*\left(\frac{(u_0^2)}{v}\right)^{\frac{1}{3}},\ Z = z^*\left(\frac{(u_0^2)}{v^2}\right)^{\frac{1}{3}},$$

$$\theta = \frac{T^* - T_\infty^*}{T_w^* - T_\infty^*},\ Gr = \frac{f\beta(T_w^* - T_\infty^*)}{u_0},\ C = \frac{C^* - C_\infty^*}{C_w^* - C_\infty^*},\ Gc = \frac{g\beta(C^* - C_\infty^*)}{C_w^* - C_\infty^*},$$

$$Pr = \frac{\mu C_p}{k},\ k = K_1\left(\frac{v}{u_0^2}\right)^{\frac{1}{3}},\ Sc = \frac{v}{D},\ M^2 = \frac{\sigma B_0^2}{\rho}\left(\frac{v}{u_0^2}\right)^{\frac{1}{3}}. \tag{6}$$

From the above, it is clear that we should determine the values of thermal layer transfer and proportionate heat transfer when measuring velocity since *Pr* is the ratio between momentum and thermal diffusivity. The heat transfer known as the *Grashof number* calculates the buoyancy to viscosity ratio. Since the buoyant force, as opposed to the viscous force, is mostly responsible for the convection, it is appropriate to measure the fluid to demonstrate this.

To examine the diffusion coefficient, use Schmidt as the ratio between mass diffusivity and momentum. First order chemical reaction on flow past a

parabolic with rotation is shown using coupled partial differential equations. Complex velocity $q = u + iv$ was used to solve equations (1) and (2), which were then combined into one equation:

$$\frac{\partial q}{\partial t} = Gr\theta + GcC + \frac{\partial^2 q}{\partial z^2} - mq, \text{ where } m = \frac{M^2}{(1+h_i)},$$

$$\frac{\partial \theta}{\partial t} = \frac{1}{Pr}\frac{\partial^2 \theta^*}{\partial z^{*2}} - R\theta^* + Q\theta^*,$$

$$\frac{\partial C}{\partial t} = \frac{1}{Sc}\frac{\partial^2 C^*}{\partial z^2} - kC \tag{7}$$

with conditions

$$q = 0,\ \theta = 0,\ C = 0 \text{ for all } z,\ t \le 0,$$

$$q = t^2,\ \theta = 1,\ C = 1 \text{ for all } z,\ t = 0,$$

$$q \to 0,\ \theta \to 0,\ C \to 0 \text{ as } z \to \infty. \tag{8}$$

3. Elucidation of the Problem

Solving equation (7) using (8) with the aid of Laplace transforms, we obtain

$$q(z) = \left\{ \begin{array}{l} \left[\frac{\eta^2 t}{m} + t^2\right]\frac{1}{2}\left[\begin{array}{l} e^{2\eta\sqrt{t}\sqrt{m}}\, erfc(\eta - \sqrt{mt}\,) \\ \quad + e^{2\eta\sqrt{t}\sqrt{m}}\, erfc(\eta + \sqrt{mt}\,) \end{array}\right] \\ \left[\frac{1}{4m} - t\right]\frac{2\eta\sqrt{t}}{2\sqrt{m}}\left[\begin{array}{l} e^{-2\eta\sqrt{t}\sqrt{m}}\, erfc(\eta - \sqrt{mt}\,) \\ \quad - e^{2\eta\sqrt{t}\sqrt{m}}\, erfc(\eta + \sqrt{mt}\,) \end{array}\right] \\ \quad - \frac{2}{m}\sqrt{\frac{t}{\pi}}e^{\left(\frac{-z^2}{4t} - mt\right)} \end{array} \right\}$$

$$-\frac{Gr}{a(1-Pr)}\left\{\begin{array}{l}\frac{e^{at}}{2}\left[\begin{array}{l}e^{-2\eta\sqrt{t}\sqrt{a+m}}\,erfc(\eta-\sqrt{(a+m)t}\,)\\ \quad+e^{2\eta\sqrt{t}\sqrt{a+m}}\,erfc(\eta+\sqrt{(a+m)t}\,)\end{array}\right]\\ -\frac{1}{2}\left[\begin{array}{l}e^{-2\eta\sqrt{t}\sqrt{m}}\,erfc(\eta-\sqrt{mt}\,)\\ \quad+e^{2\eta\sqrt{t}\sqrt{m}}\,erfc(\eta+\sqrt{mt}\,)\end{array}\right]\end{array}\right\}$$

$$-\frac{Gs}{b(1-Sc)}\left\{\begin{array}{l}\frac{e^{at}}{2}\left[\begin{array}{l}e^{-2\eta\sqrt{t}\sqrt{b+m}}\,erfc(\eta-\sqrt{(b+m)t}\,)\\ \quad+e^{2\eta\sqrt{t}\sqrt{b+m}}\,erfc(\eta+\sqrt{(b+m)t}\,)\end{array}\right]\\ -\frac{1}{2}\left[\begin{array}{l}e^{-2\eta\sqrt{t}\sqrt{m}}\,erfc(\eta-\sqrt{mt}\,)\\ \quad+e^{2\eta\sqrt{t}\sqrt{m}}\,erfc(\eta+\sqrt{mt}\,)\end{array}\right]\end{array}\right\}$$

$$+\frac{Gr}{a(1-Pr)}\left\{\begin{array}{l}\frac{e^{at}}{2}\left[\begin{array}{l}e^{-2\eta\sqrt{t}\sqrt{Pr(a+R-Q)}}\,erfc(\eta\sqrt{Pr}-\sqrt{(a+R-Q)t}\,)\\ \quad+e^{2\eta\sqrt{t}\sqrt{Pr(a+R-Q)}}\,erfc(\eta\sqrt{Pr}+\sqrt{(a+R-Q)t}\,)\end{array}\right]\\ -\frac{1}{2}\left[\begin{array}{l}e^{-2\eta\sqrt{t}\sqrt{Pr(R-Q)}}\,erfc(\eta\sqrt{Pr}-\sqrt{(R-Q)t}\,)\\ \quad+e^{2\eta\sqrt{t}\sqrt{Pr(R-Q)}}\,erfc(\eta\sqrt{Pr}+\sqrt{(R-Q)t}\,)\end{array}\right]\end{array}\right\}$$

$$+\frac{Gc}{b(1-Sc)}\left\{\begin{array}{l}\frac{e^{bt}}{2}\left[\begin{array}{l}e^{-2\eta\sqrt{t}\sqrt{Sc(b+k)}}\,erfc(\eta\sqrt{Sc}-\sqrt{(b+k)t}\,)\\ \quad+e^{2\eta\sqrt{t}\sqrt{Sc(b+k)}}\,erfc(\eta\sqrt{Sc}+\sqrt{(b+k)t}\,)\end{array}\right]\\ -\frac{1}{2}\left[\begin{array}{l}e^{-2\eta\sqrt{t}\sqrt{Sck}}\,erfc(\eta\sqrt{Sc}-\sqrt{kt}\,)\\ \quad+e^{2\eta\sqrt{t}\sqrt{Sck}}\,erfc(\eta\sqrt{Sc}+\sqrt{kt}\,)\end{array}\right]\end{array}\right\}, \tag{9}$$

$$\theta=\frac{1}{2}[e^{-2\eta\sqrt{Pr}\sqrt{(R-Q)t}}\,erfc(\eta\sqrt{Pr}-\sqrt{(R-Q)t}\,)$$

$$+e^{2\eta\sqrt{Pr}\sqrt{(R-Q)t}}\,erfc(\eta\sqrt{Pr}+\sqrt{(R-Q)t}\,)], \tag{10}$$

$$C=\frac{1}{2}[e^{-2\sqrt{\eta}\sqrt{Sck}}\,erfc(\eta\sqrt{Sc}-\sqrt{kt}\,)+e^{2\sqrt{\eta}\sqrt{Sck}}\,erfc(\eta\sqrt{Sc}+\sqrt{kt}\,)]. \tag{11}$$

4. Results and Discussion

The velocity for changing values of k, Sc, Pr, Gr, Gc, h, R and Q has been presented in the diagrams given in this section.

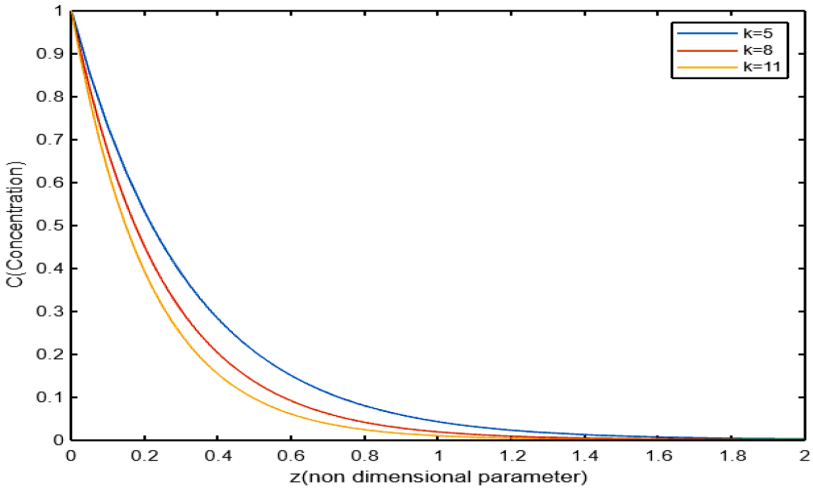

Figure 1. Concentration profile for many k values, including 5, 8, and 11. As chemical reaction k grows, concentration decreases.

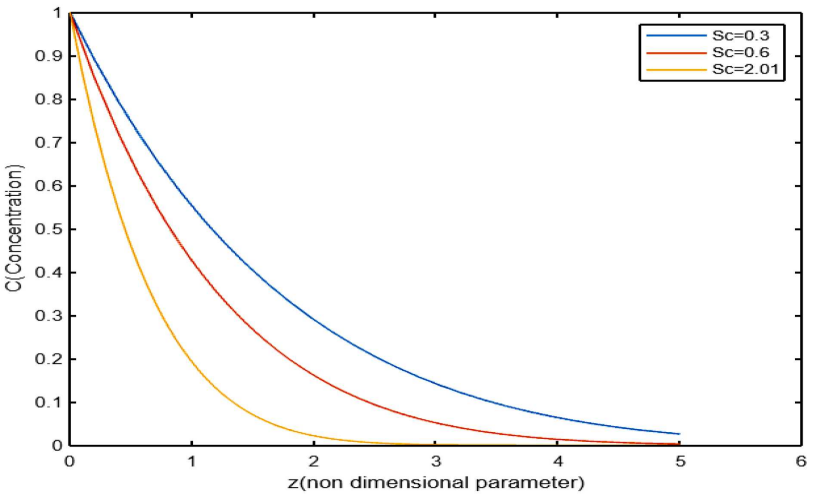

Figure 2. It shows the Sc concentration profile. Concentration decreases as the Schmidt number increases, for various values of $Sc = 0.3$, 0.6 and 2.01.

Figures 1 and 2 show the concentration profiles.

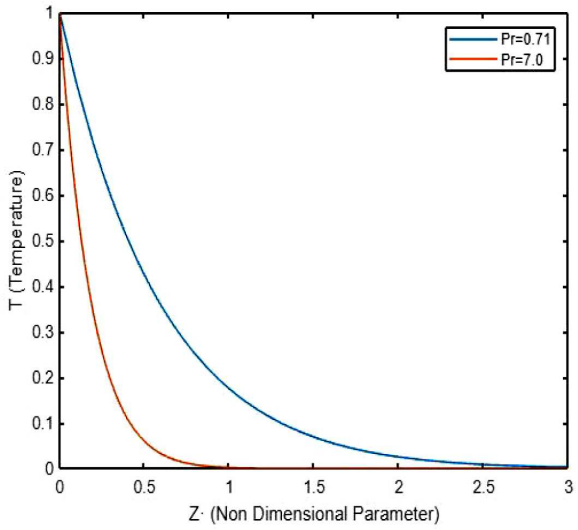

Figure 3. Temperature profile for $Pr = 0.71, 7.0$. Temperature shrinks when Prandtl number Pr hikes.

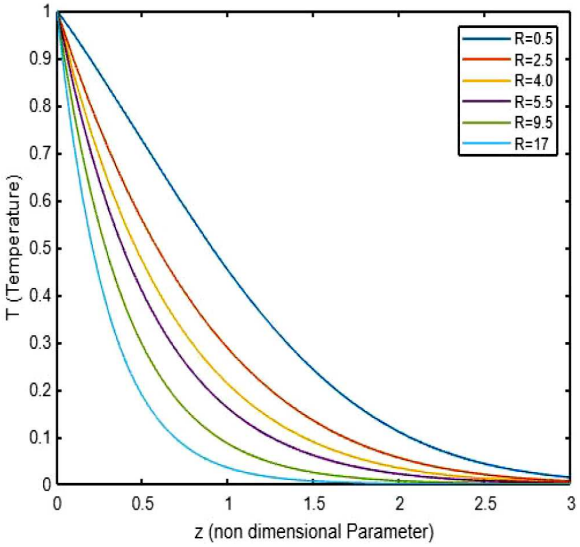

Figure 4. Temperature profile for $R = 0.5, 2.5, 4.0, 5.5, 9.5, 17$. Temperature shrinks when radiation R rises.

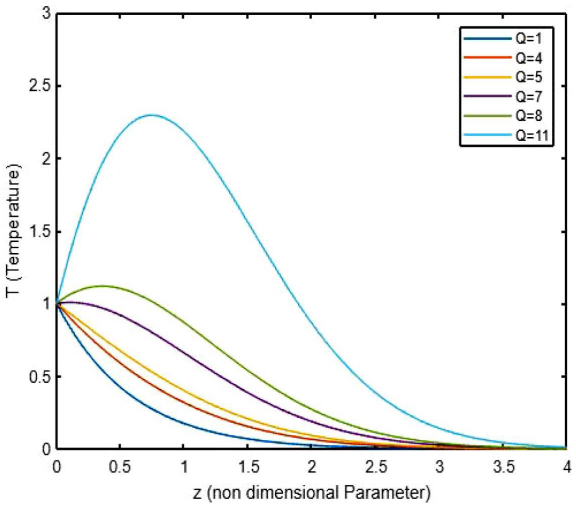

Figure 5. Temperature profile for $Q = 1, 4, 5, 7, 8, 11$. Temperature rises when heat source Q rises.

In Figures 3, 4 and 5, the temperature profiles are depicted.

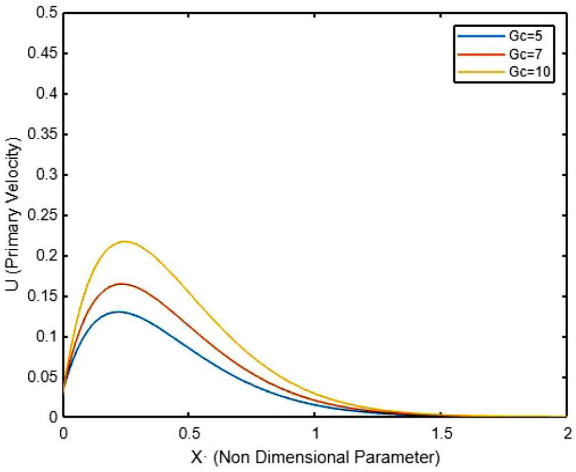

Figure 6. PV for $Gc = 5, 7, 10$. The velocity rises when mass Grashof number Gc hikes.

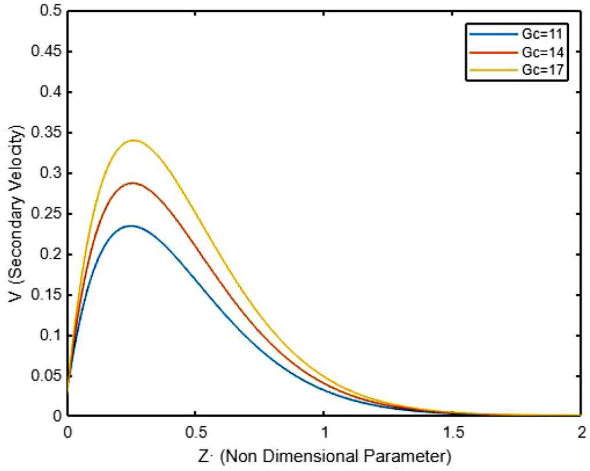

Figure 7. SV for $Gc = 11, 14, 17$. The velocity rises when mass Grashof number Gc hikes.

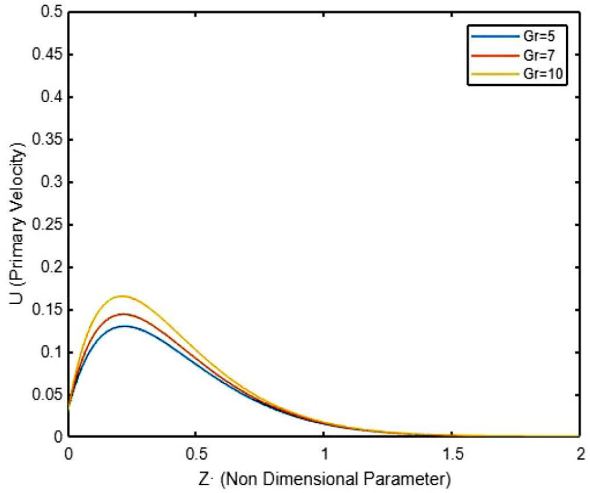

Figure 8. PV for $Gr = 5, 7, 10$. The velocity increases when thermal Grashof values rise.

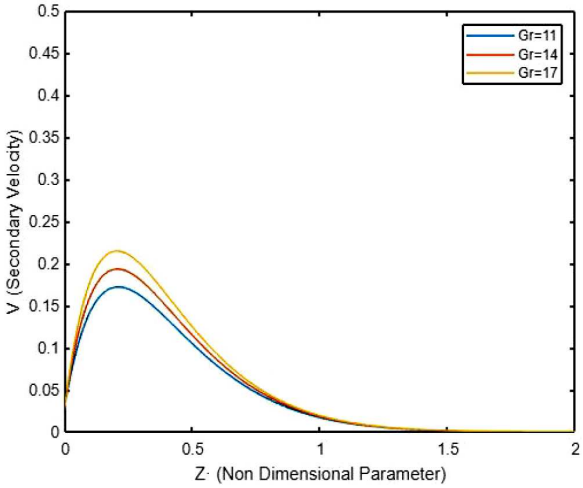

Figure 9. SV for $Gr = 11, 14, 17$. The velocity rises when thermal Grashof values rise.

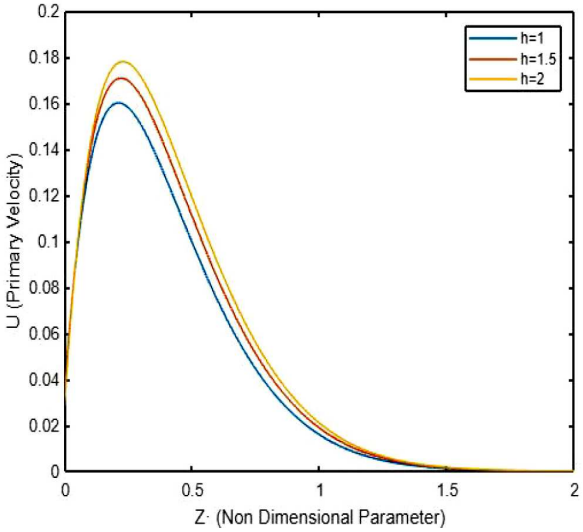

Figure 10. PV for $h = 1, 1.5, 2$. The velocity rises when heat source rises.

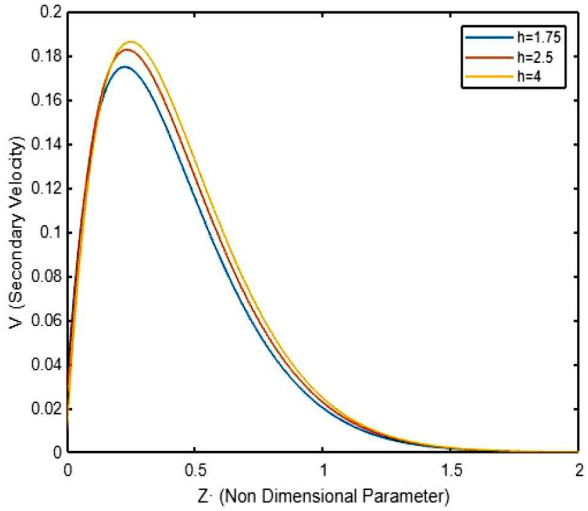

Figure 11. SV for $h = 1.75, 2.5, 4$. The velocity rises when heat source rises.

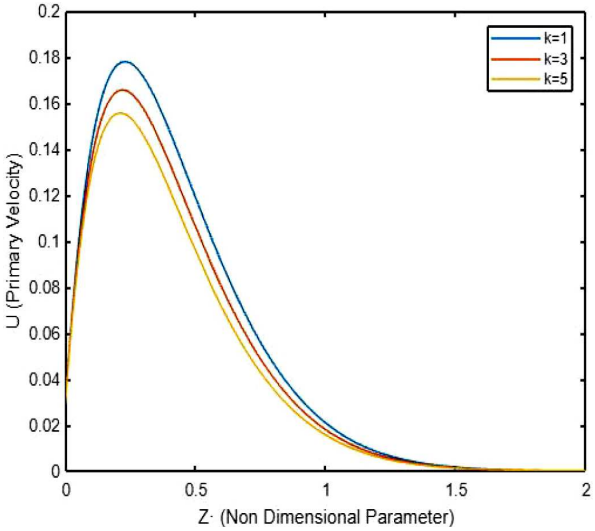

Figure 12. PV for $k = 1, 3, 5$. The velocity reduces when k rises.

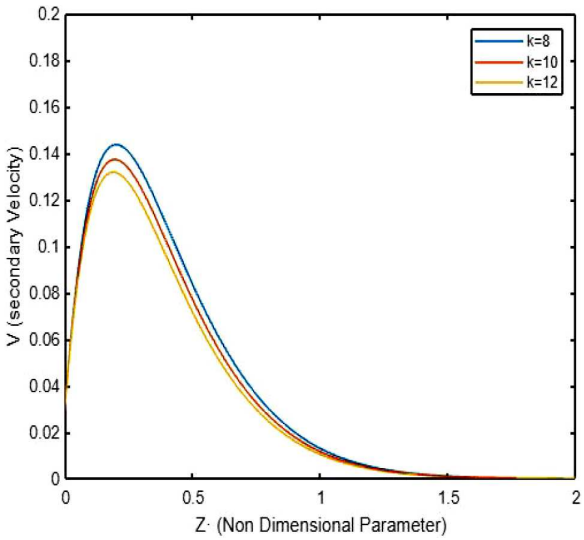

Figure 13. SV for $k = 8, 10, 12$. The velocity reduces when k rises.

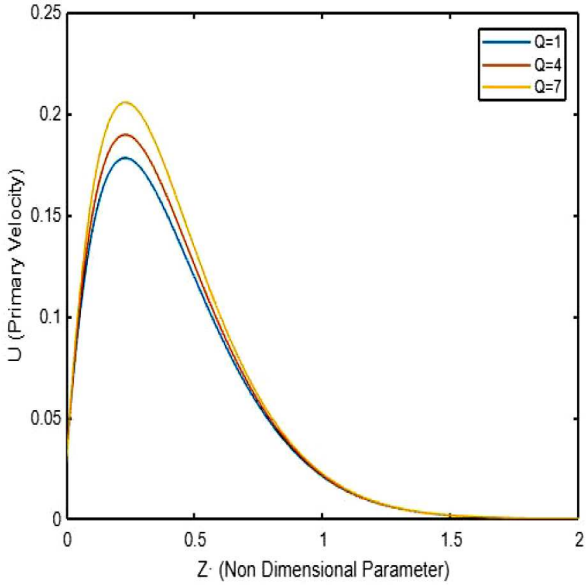

Figure 14. PV for $Q = 1, 4, 7$. The velocity reduces when heat source rises.

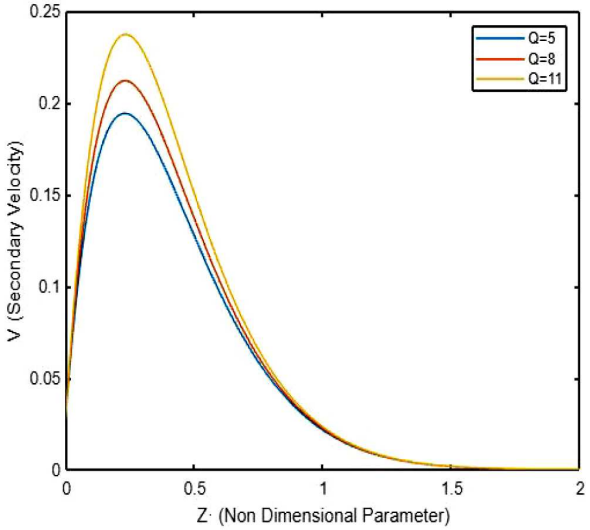

Figure 15. SV for $Q = 5, 8, 11$. The velocity reduces when heat source rises.

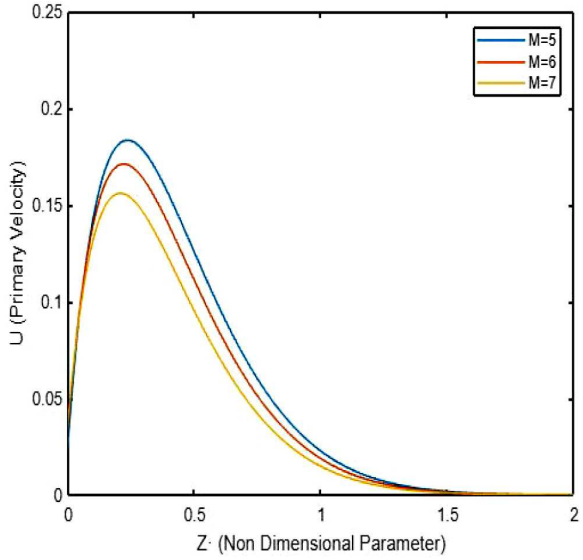

Figure 16. PV for $M = 5, 6, 7$. The velocity reduces with increasing Hartmann number.

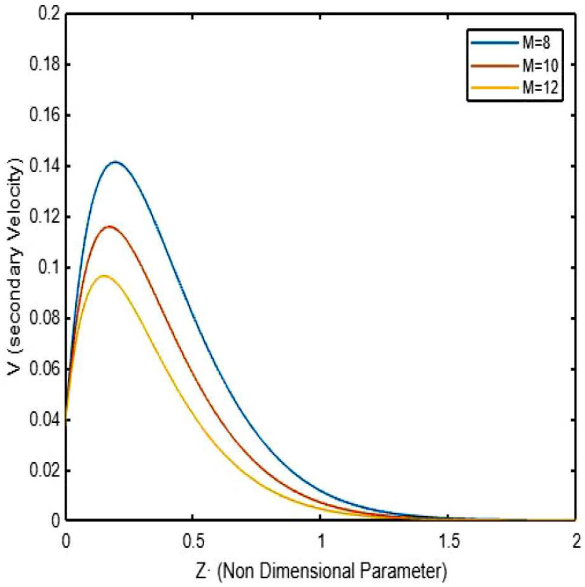

Figure 17. SV for $M = 8, 10, 12$. The velocity decreases with increasing Hartmann number.

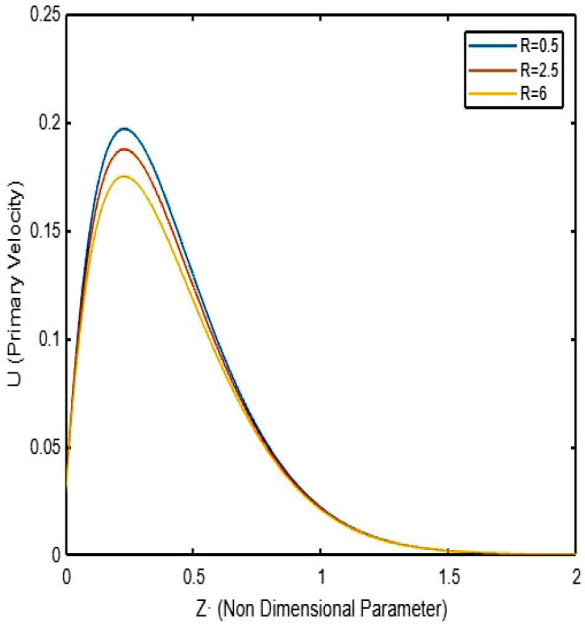

Figure 18. PV for different values of R. The velocity reduces when R rises.

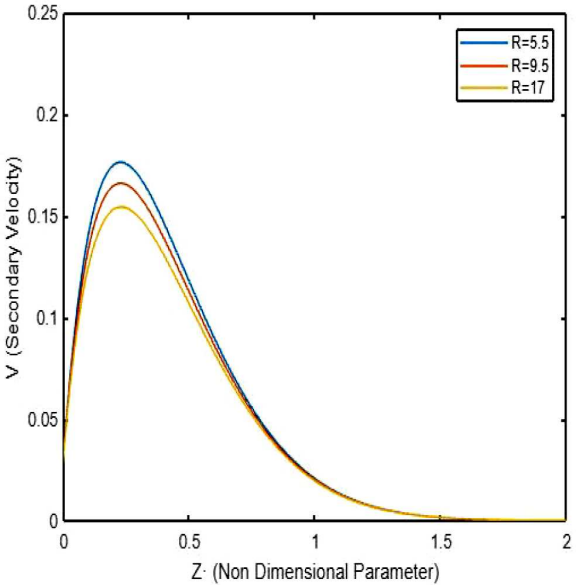

Figure 19. SV for $R = 5.5, 9.5, 17$. The velocity reduces when R rises.

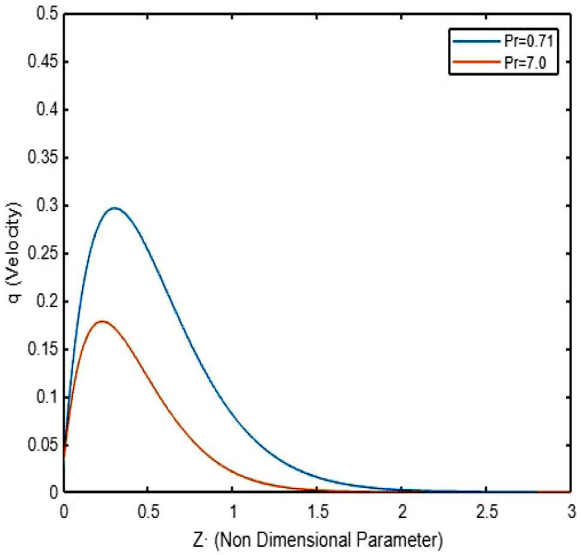

Figure 20. Velocity for $Pr = 0.71, 7.0$. The velocity reduces when Prantdl number Pr rises.

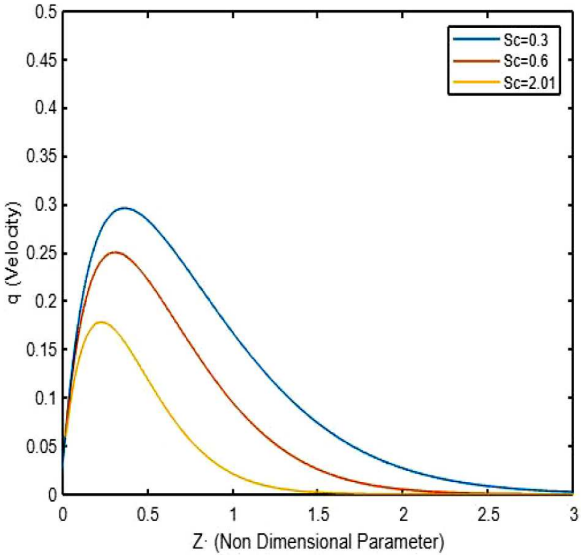

Figure 21. Velocity for Sc = 0.3, 0.6, 2.01. The velocity reduces when Schmidt (Sc) number rises.

In Figures 6 to 21, the velocity profiles are depicted.

5. Tabulation

Table 1. The estimated concentration profile

Non-dimensional parameter	Figure 1	Figure 2
	Concentration k	Concentration Sc
Gr	7	7
Gc	7	7
Pr	0.71	0.71
R	5	5
Q	1	1
M	5.5	5.5
h	2	2
Sc	2.01	0.3, 0.6, 2.01
k	5, 8, 11	1
t	1	1

Table 2. Numerical estimated temperature profiles for several values of *Pr*, *R*, and *Q*

Non-dimensional parameters	Figure 3	Figure 4	Figure 5
	Temperature *Pr*	Temperature *R*	Temperature *Q*
Gr	7	7	7
Gc	7	7	7
Pr	0.71, 7.0	0.71	0.71
R	5	5, 10, 15	5
Q	1	1	2, 3, 4
M	5.5	5.5	5.5
h	2	2	2
Sc	2.01	2.01	2.01
k	1	1	1
t	0.5	0.5	0.5

Table 3. Numerical estimated concentration profiles for several values of *Gc* and *Gr*

Non-dimensional parameters	Figure 6	Figure 7	Figure 8	Figure 9
	Primary velocity *Gc*	Secondary velocity *Gc*	Primary velocity *Gr*	Secondary velocity *Gr*
Gr	7	7	**5, 7, 10**	**11, 14, 17**
Gc	**5, 7, 10**	**11, 14, 17**	7	7
Pr	0.71	0.71	0.71	0.71
R	5	5	5	5
Q	1	1	1	1
M	5.5	5.5	5.5	5.5
h	2	2	2	2
Sc	2.01	2.01	2.01	2.01
k	1	1	1	1
t	1	1		

Table 4. Numerical estimated concentration profiles for several values of h and k

Non-dimensional parameters	Figure 10	Figure 11	Figure 12	Figure 13
	Primary velocity h	Secondary velocity h	Primary velocity k	Secondary velocity k
Gr	7	7	7	7
Gc	7	7	7	7
Pr	0.71	0.71	0.71	0.71
R	5	5	5	5
Q	1	1	1	1
M	5.5	5.5	5.5	5.5
h	**1, 1.5, 2**	**1.75, 2, 4**	2	2
Sc	2.01	2.01	2.01	2.01
k	1	1	**1, 3, 5**	**8, 10, 12**
t	0.2	0.2	0.2	0.2

Table 5. Numerical estimated concentration profiles for several values of Q and R

Non-dimensional parameters	Figure 14	Figure 15	Figure 16	Figure 17
	Primary velocity Q	Secondary velocity Q	Primary velocity M	Secondary velocity M
Gr	7	7	7	7
Gc	7	7	7	7
Pr	0.71	0.71	0.71	0.71
R	5	5	5.0	5.0
Q	**1, 4, 7**	**5, 8, 11**	1	1
M	5.5	5.5	**5, 6, 7**	**8, 10, 12**
h	2	2	2	2
Sc	2.01	2.01	2.01	2.01
k	1	1	1	1
t	0.2	0.2	0.2	0.2

Table 6. Numerical values for estimated velocity profiles for varying *M*, *Sc* and *Pr* values

Non-dimensional parameters	Figure 18	Figure 19	Figure 20	Figure 21
	Primary velocity *R*	Secondary velocity *R*	Primary velocity *Pr*	Secondary velocity *Sc*
Gr	7	7	7	7
Gc	7	7	7	7
Pr	0.71	0.71	**0.71, 7.0**	0.71
R	**0.5, 2.5, 6**	**5.5, 9.5, 17**	5	5
Q	1	1	1	1
M	5.5	5.5	5.5	5.5
h	2	2	2	2
Sc	2.01	2.01	2.01	**0.3, 0.6, 2.01**
k	1	1	1	1
t	0.2	0.2	0.2	0.2

6. Conclusion

As this is a variational study from the literature involving accelerated isothermal vertical plate with the basic HMT aspects, this provides a simple and nice platform for computational work and based on the calculations, we could conclude that

(i) Velocity reduces when radiation '*R*' rises,

Velocity reduces when Hartmann number *M* rises and

Velocity rises when Grashof '*Gc*' and '*Gr*' values rise,

Velocity rises when heat source '*Q*' rises,

Velocity rises when Hall current '*h*' rises.

(ii) Temperature falls when radiation '*R*' rises and

Temperature rises when heat source '*Q*' rises.

(iii) Concentration reduces when chemical reaction '*k*' increases.

So, we are able to achieve an extended list of conclusions by the variation and we intend to enhance the study by including more parameters in our future study.

Acknowledgement

The authors thank the anonymous referees for their valuable suggestions and comments which improved the paper.

References

[1] U. N. Das, R. K. Deka and V. M. Soundalgekar, Effects of mass transfer on flow past an impulsively started infinite vertical plate with constant heat flux and chemical reaction, Forschung im Ingenieurwesen 60(10) (1994), 284-287.

[2] R. Muthucumaraswamy, Effects of a chemical reaction on a moving isothermal vertical surface with Suction, Acta Mechanica 155 (2022), 65-70.

[3] M. N. Sarki and A. Ahmed, Heat and mass transfer with chemical reaction and exponential mass diffusion, International Journal of Engineering Research and Technology (IJERT) 1(8) (2012), 1-12.

[4] M. Thamizhsudar, R. Muthucumaraswamy and A. K. Bhuvaneswari, Heat and mass transfer effects on MHD flow past an exponentially accelerated vertical plate in the presence of rotation and Hall current, Journal of Advance Research in Dynamical and Control Systems 9 (2017), 73-82.

[5] S. Dilip Jose and A. Selvaraj, Convective, heat and mass transfer effects of rotation on parabolic flow past an accelerated isothermal vertical plate in the presence of chemical reaction of first order, JP Journal of Heat and Mass Transfer 24(1) (2021), 191-206.

[6] J. Uwanta and Murtala Sani, Heat mass transfer flow past an infinite vertical plate with variable thermal conductivity, Heat Source and Chemical Reaction, The International Journal of Engineering and Science (IJES) 3 (2014), 77-89.

[7] D. Maran, A. Selvaraj, M. Usha and S. Dilip Jose, First order chemical response impact of MHD flow past an infinite vertical plate within sight of exponentially with variable mass diffusion and thermal radiation, Materials Today : Proceedings 46 (2021), 3302-3307.

[8] K. Rachna, Unsteady MHD flow, heat and mass transfer along an accelerated vertical porous plate in the influence of viscous dissipation, heat source and variable suction, International Journal of Mathematics and Computer Applications Research 3(1) (2013), 229-236.

[9] M. S. Abel and N. Mahesha, Effects of thermal buoyancy and variable thermal conductivity in a power law fluid past a vertical stretching sheet in the presence of non uniform heat source, Internat. J. Non-Linear Mech. 44 (2009), 1-12.

[10] M. Ferdows, M. A. Sattar and M. N. A. Siddiki, Numerical approach on parameters of the thermal radiation interaction with convection in boundary layer flow at a vertical plate with variable suction, Thammasat International Journal of Science and Technology 9 (2004), 19-28.

[11] M. Acharya, G. C. Dash and L. P. Singh, Effect of chemical and thermal diffusion with Hall current on unsteady hydromagnetic flow near an infinite vertical porous plate, Journal of Applied Physics 28 (1995), 2455-2464.

[12] P. G. Siddheshwar and U. S. Mahabaleshwar, Effect of radiation and heat source on MHD flow of a viscoelastic liquid and heat transfer over a stretching sheet, Internat. J. Non-Linear Mech. 40 (2005), 807-820.

[13] P. R. Sharma and G. Singh, Unsteady MHD free convective flow and heat transfer along a vertical porous plate with variable suction and internal heat generation, International Journal of Applied Mathematics and Mechanics 4 (2008), 1-8.

[14] R. Muthucumaraswamy and E. Geetha, Effects of parabolic motion of an isothermal vertical plate with constant mass flux, Ain Shams Engineering Journal 5 (2014), 1317-1323.

[15] R. Hetnarski, On inverting the Laplace transforms connected with the error function, Appl. Math. 7(4) (1964), 399-405.

[16] R. B. Hetnarski, An algorithm for generating some inverse Laplace transform of exponential form, ZAMP 26 (1975), 249-253.